Modeling magnetic circular dichroism within the polarizable embedding approach

Nørby, Morten Steen; Coriani, Sonia; Kongsted, Jacob

Published in:
Theoretical Chemistry Accounts

Link to article, DOI:
10.1007/s00214-018-2220-5

Publication date:
2018

Document Version
Peer reviewed version

Noname manuscript No.
(will be inserted by the editor)

Modeling Magnetic Circular Dichroism within the Polarizable Embedding Approach

Morten Steen Nørby · Sonia Coriani · Jacob Kongsted

Received: date / Accepted: date

Abstract Magnetic circular dichroism (MCD) is defined as the differential absorption of left and right circularly polarized light in a sample subjected to an external magnetic field. In order to interpret the results of MCD measurements, theoretical predictions of key MCD parameters can be of utmost importance. From an experimental point of view, MCD spectra of molecules are often measured in an environment and most notably in a solution. Thus, it may be very important that the method used to predict the MCD parameters is able to correctly account for medium effects. In this paper we investigate the quality of MCD calculations within the Polarizable Embedding approach, which represents a fully atomistic and polarizable representation of an environment surrounding a smaller region treated using quantum mechanics. Furthermore, we compare the performance of the Polarizable Embedding scheme to the use of the more conventional dielectric continuum approach. Results are presented for cytosine and hypoxanthine solvated in water.

Keywords Magnetic Circular Dichroism · Polarizable Embedding · Solvation effects

1 Introduction

Magnetic circular dichroism (MCD) is a spectroscopic method of high importance in relation to determination of electronic structures of both ground and excited states.[1,2] Experimentally, MCD originates from measurements

Morten Steen Nørby
Department of Physics, Chemistry and Pharmacy, University of Southern Denmark, 5230 Odense M. Denmark. E-mail: mortennp@sdu.dk

Sonia Coriani, Department of Chemistry, Technical University of Denmark, Kemitorvet, Build. 207, 2800 Kongens Lyngby, Denmark. E-mail: soco@kemi.dtu.dk · Jacob Kongsted, Department of Physics, Chemistry and Pharmacy, University of Southern Denmark, 5230 Odense M. Denmark. E-mail: kongsted@sdu.dk

of the differential absorption of left and right hand circularly polarized light in the presence of an applied magnetic field.[1,3] Due to the signed nature of the MCD signal, MCD can often reveal states that would otherwise not be observed in conventional one-photon absorption (OPA) spectroscopy, such as UV/Vis. Typically, the MCD spectrum is analyzed in terms of three different contributions, known as the Faraday A, B and C terms.[4,5,6,7,8,9,10] While only the A and B terms contribute to the MCD spectrum of closed-shell molecules, the C term is also present for open-shell system. Furthermore, the A term is only found if the molecule possesses degenerate excited states. Thus in many practical cases it is sufficient to consider only the B term.

Today, quantum chemical calculations of spectroscopic parameters can be extremely useful for the interpretation of experimental measurements. Regarding MCD, efficient computational protocols for determining the individual MCD terms were introduced within the response function theory formalism, based on either a Hartree-Fock[11], multiconfigurational self-consistent field (MCSCF)[11] or Coupled Cluster[12,13] wave function parametrizations. However, as these methods either lack electron correlation or are often computationally too demanding to be applied for larger molecules, the method of choice has become time-dependent density functional theory (TD-DFT).[14, 15,16,17,18,19,20,21,22,23] The conventional procedure consists in using such electronic structure methods to calculate the Faraday terms relevant for MCD, and then use these molecular properties in combination with Lorentzian band profiles to simulate the MCD spectrum. However, the MCD spectrum may also be determined directly with use of the complex polarization propagator (CPP) method developed by Norman and coworkers. [24,25,26,27,28,29] The CPP approach introduces a finite lifetime of the excited states directly in the response calculations, thereby avoiding the unphysical divergence of the standard response equations at resonance frequencies. By this, the CPP equations are well-defined throughout the entire spectral region. A somewhat similar approach for MCD was presented by Krykunov *et al.* in 2007.[30]

In order to compare predicted and measured spectra directly, one must of course carefully consider how to represent the system when performing the theoretical calculations. A major issue in this respect is that experimental results are typically obtained from measurements in a solution. Therefore, a proper description of the environmental effects is a key component for predicting reliable spectroscopic parameters. Regarding computation of MCD parameters, environmental effects have previously been included using either a polarizable continuum model (PCM)[18] and/or by including a small number of solvent molecules in the QM description, the so-called super-molecular approach[31, 29,32]. One advantage of using a PCM approach to model the effects of the solvent is that the solvent dynamics is implicitly included. From a computational point of view, this means that calculation of the MCD parameters – including solvation effects – may be processed by a single electronic structure calculations in complete analogy to the case of the molecule in isolation. However, PCM neglects per definition inclusion of specific intermolecular interactions. The latter can be introduced by use of the super-molecular approach, but at an

increased computational cost. Moreover, since environmental effects are usually very long-ranged, it can be necessary to either include a large amount of solvent molecules in the quantum region or embed a smaller portion of solvent molecules in a continuum to reach convergence of the spectroscopic parameter with respect to the number of solvent molecules included in the quantum region.[33,34,35,36]

Another strategy to include environmental effects is through the QM/MM approach.[37] Here, all details of the structure of the environment are kept, but, in contrast to the super-molecular approach, the environmental effects are accounted for via the much less computational demanding molecular mechanics (MM) approach. This means that it is possible to include much larger environments into the electronic structure calculations.

In this paper we will – to our knowledge – for the first time use a (polarizable) QM/MM response theory approach to simulate a MCD spectrum. In detail, we will apply the Polarizable Embedding (PE) approach coupled with the CPP method.[38,39,40] For earlier works along the line of magnetic and higher order response properties in a QM/MM response picture we refer to Refs. [41,42]. Central to the PE approach, and any QM/MM approach, is the quality of the parameters used to represent the environment – that is, the embedding potential. To mimic the permanent electrostatics, a common choice is to use an atom centered multipole expansion truncated at a given order, which is also the strategy followed in the PE model. Furthermore, inclusion of polarization increases the accuracy of the embedding, since the environment is allowed to respond not only to changes in the electronic structure part of the system, but also to the inhomogeneity of the environment itself.[37,43,44,45,38,39,46,47,48,49,50,51,52,53,54,55,56,57,58,59,60] In this paper our focus is solely centered on the induced dipole model. In recent papers we have shown that an accurate embedding potential allows for use of much smaller quantum regions without compromising the accuracy of the final predicted spectroscopic observables. In this way, efficient calculations over a large number of snapshots become possible in order to address the issue of conformational sampling.[36,61,62]

The MCD spectra of the nucleobases occurring in DNA have been studied both from a theoretical and an experimental point of view, where the theoretical results typically have been used to assign and interpret the experimentally recorded spectrum.[29,63,64,65,31] In a recent paper, the MCD spectra of various nucleobases have been calculated by means of quantum chemical methods based on TDDFT calculations.[29] Especially the role of solvent effects – included either through use of the PCM or super-molecular approach – was discussed, and it was found that the intensities for the MCD signal typically show an enhancement compared to similar calculations for the molecule in isolation.

In addition, the inclusion of local fields in the embedding formalism can be crucial and may significantly alter the response and transition properties of the embedded molecule – a point that so far has not been addressed in relation to calculation of MCD parameters. Local fields have previously been

introduced in the framework of PCM and are here commonly known as cavity field (CF) effects.[66] Yet, only recently has the equivalent to the CF effect been introduced in the PE model.[67] It goes under the name of effective external field (EEF) effect, and it has so far been applied to linear absorption properties such as electronic circular dicroism[36] and one- and two-photon absorption properties.[67,68] Here we extend the analysis of local fields within the PE model to CPP quadratic response functions, exemplified by the calculation of MCD spectra. In addition, we will compare the use of the PE model to the use of a continuum model. Specifically, we here consider the FixSol model,[69] which belongs to the family of conductor-like screening models (COSMO).[70, 71,72,73,74] CF effects have recently been introduced in the FixSol model[36], thus allowing for a direct comparison of the intensities originating from both PE and FixSol solvent models.

2 Theory

As discussed in the introduction, the MCD response can be interpreted in terms of the three Faraday parameters (A, B and C terms). However, since the molecules considered in this paper are all closed shell molecules with no degenerate excited states, only the B term is of relevance. Thus, the differential absorption (in the absence of the A and C terms) of right and left circularly polarized light of a sample of randomly oriented molecules in the presence of an external magnetic field is calculated in terms of the molar decadic coefficient, given by

$$\Delta\epsilon(\omega) = -\frac{8\pi^2 N_A \omega B_{\text{ext}}}{3 \times 1000 \times \ln(10)(4\pi\epsilon_0)\hbar c_0} \sum_j a_j(\omega) B(0 \to j) \ . \tag{1}$$

Here ω is the frequency of the external perturbation, while the line shape function yielding the spectral broadening is assumed of Lorentzian form

$$a_j(\omega) = \frac{1}{\pi} \frac{\gamma}{(\omega_j - \omega)^2 + \gamma^2} \ . \tag{2}$$

In this expression ω_j is the excitation energy corresponding to the transition from the ground state 0 to the excited state j ($0 \to j$). From a computational point of view, the molar decadic coefficient can be more conveniently expressed in terms of the real part of the mixed magnetic/electric damped quadratic response function

$$\Delta\epsilon(\omega) = -\frac{8\pi^2 N_A \omega B_{\text{ext}}}{3 \times 1000 \times \ln(10)(4\pi\epsilon_0)\hbar c_0} \times \epsilon_{\alpha\beta\delta} \text{Re}\langle\langle \mu_\alpha; \mu_\beta; m_\delta \rangle\rangle^{\gamma}_{\omega,0} \tag{3}$$

where $\epsilon_{\alpha\beta\delta}$ is the Levi-Civita tensor, and m_α and μ_α are components of the magnetic and electric dipole operators, respectively. In the damped quadratic response function, γ is introduced as a phenomenological constant, related to the finite lifetime of the excited states. This ensures convergence of the

Fig. 1 Cytosine (left) and Hypoxanthine (right)

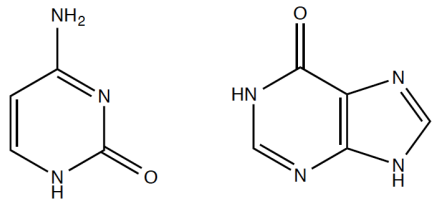

response function not only in the non-resonant part of the spectrum but also in the resonant part. The computation of the damped quadratic response function within the CPP approach requires the ability to efficiently solve complex linear response equations.[29,75,76]

To include the solvent effects in the calculation of the MCD spectra, we consider the unification of the PE model[38,39] with the CPP approach,[75, 76] resulting in the PE-CPP method.[40] The PE model utilizes an advanced embedding description where the environment surrounds a central core region treated using quantum mechanics. The environment is represented in terms of atom-centered multipole moments and an-isotropic polarizabilities. The former mimic the permanent charge distribution of the environment, whereas the latter describe the induced charge distribution of the environment. The interactions between the quantum and classical regions are described through embedding operators, that are added to the standard Kohn-Sham vacuum operator ($\hat{f}^{\mathrm{KS}}$)

$$\hat{f}^{\mathrm{eff}} = \hat{f}^{\mathrm{KS}} + \hat{v}^{\mathrm{es}} + \hat{v}^{\mathrm{ind}} \ , \tag{4}$$

where the multipole moments are used to construct the electrostatic embedding operator, $\hat{v}^{\mathrm{es}}$, and the polarizabilities are used to construct the polarization operator, $\hat{v}^{\mathrm{ind}}$. For further details regarding the construction of $\hat{v}^{\mathrm{es}}$ and $\hat{v}^{\mathrm{ind}}$, see refs [38] and [39]. The additional contributions to the damped quadratic response function in Eq. 3 stemming from the polarizable environment can be described as two separate contributions: a zeroth-order contribution, which corresponds to the static (ground-state) polarization of the environment, and a contribution that describes the dynamical response of the environment due to the change in the charge distribution of the quantum region caused by the perturbation. These two contributions enter the electronic Hessian.[77] In addition, the property gradient is also modified due to the applied perturbation,[67] leading to a modification of the local field that can potentially be crucial for calculations of transition properties of the embedded molecule.[67,36,68]

3 Computational details

All calculations of MCD spectra were carried out using a development version of the Dalton program[78] interfaced with the PE library[79] and Gen1Int[80,

81]. A common lifetime parameter γ of 1000 cm^{-1} and a frequency step of 0.0025 au were used in the CPP calculations. Both as starting structure for the MD simulations and for single structure MCD calculations we have optimized the geometries of cytosine and hypoxanthine, see Figure 1, at the B3LYP/cc-pVTZ[82,83,84] level of theory using Gaussian 09.[85] The MCD calculations of the solvated molecules are based on a number of snapshots extracted from MD simulations. For this, we have performed QM/MM MD simulations of cytosine and hypoxanthine solvated in water. The QM/MM MD simulations were carried out in the *sander* module in AMBER.[86] The simulations utilized the PM6-DH+[87] method for cytosine and hypoxanthine, while the water molecules were described using the TIP3P water model.[88, 89] Both cytosine, hypoxanthine and the water molecules were initially minimized with the conjugate gradient minimizer for 1000 steps before an initial equilibration for 50 ps in the NVT ensemble at 300 K, followed by an additional equilibration for 50 ps in the NPT ensemble at 300 K and a pressure of 1 bar. To obtain adequate sampling, each of the compounds was first run for 1 ns in the NPT ensemble. A 100 snapshots were subsequently extracted from each of the 1-ns trajectories and used as starting points for additional 2-ns simulations, for a total of 0.8 μs simulation time. The final snapshot from each trajectory was extracted, for a total of 100 snapshots used for calculating the MCD spectrum (we refer to the Supporting Information file for a detailed analysis of the MCD spectrum with respect to the number of snapshots included in the averaging). Excitation energies, oscillator strengths, and MCD signals were computed at the PE(EFF)-DFT level of theory, utilizing the CAMB3LYP exchange-correlation functional[90]. The aug-cc-pVDZ basis set[91] was adopted for the heavy atoms, whereas the cc-pVDZ basis set[91] was used for the H atoms. For the subsequent PE calculations, we have included 100 water molecules nearest the solute to define the environment. We refer to the supporting information file for additional basis set studies and for an analysis of the convergence of the MCD spectrum with respect to the number of water molecules included in the environment. The embedding potential representing the solvent molecules (water) consists of distributed multipole moments up to 2nd order (quadrupoles) and distributed anisotropic dipole-dipole polarizabilities. The expansion centers for the distributed multipoles and polarizabilities were placed at the atomic nuclei that define the environment. All distributed multipoles and polarizabilities were derived by utilizing the LoProp approach[92] employing the LoProp for Dalton script[93] based on integrals and response functions obtained from the Dalton program package.[78] In addition, we also consider the standard embedding potential constructed from the TIP3P water model.[88,89]

When using the continuum model (FixSol) to incorporate the effects of solvation in the calculation of MCD parameters, atomic radii of 1.40, 2.10 and 1.90 Å were used for the H, C, and O atoms, respectively, to define the molecular cavity. For the ground-state wave function optimization, we used a static dielectric constant of $\epsilon = 78.39$, whereas for the transition property calculations we used $\epsilon_{\text{inf}} = 1.776$.

4 Results

4.1 Cytosine

The first system to be considered is cytosine in water solution. The experimental MCD spectrum of cytosine is dominated by two negative peaks – one at 265 nm and a second peak at 236 nm.[63] We note that Kaito *et al.*[94] also measured the MCD spectrum of cytosine (see supporting information Fig. S-5). However, for reasons not clear to us the intensities in this spectrum are significantly enhanced compared to our calculations and the spectrum obtained by Voelter *et al.*[63]

Figure 2 shows the MCD spectrum of cytosine computed from a single structure of cytosine. The MCD spectrum has been computed either for cytosine in isolation (vacuum) or based on a continuum solvation model (FixSol) both including or excluding cavity field effects (CF). Shown in the same figure is also the experimental MCD spectrum recorded in a water solution. It is clear from Figure 2 that the positions of the peaks are blue shifted for the computed spectra compared to the experimental spectrum. Furthermore, when including solvent effects through the dielectric continuum model, the intensities become significantly overestimated. This finding is in perfect agreement with previous observations by Fahleson *et al.*[29] Also, as seen from Figure 2, inclusion of cavity field effects into the continuum description lead for both signals to a slight increase in the intensity. The peak separation is not affected by inclusion of cavity field effects, since this only gives rise to changes in the absorption strengths. Including the solvent effects through the continuum model calculated from a single optimized structure indeed leads to a decrease in peak separation compared to vacuum, i.e. from 0.936 eV to 0.830 eV (see Table 1), bringing the predictions in better agreement with the experimental results, thus emphasizing the importance of solvent effects.

In Figure 3 we present the MCD spectra computed using different solvation models. These spectra have been obtained by averaging over the 100 snapshots extracted from the MD simulations, as discussed in Sec. 3 The spectra thereby include nuclear dynamical effects caused by finite temperature. Compared to the use of a single geometry optimized structure (Figure 2), we observe that the intensities of the computed spectra are now much more in line with the experimental counterparts. Furthermore, the peak separation is also improved compared to the single-structure results. We here note that inclusion of explicit solvent molecules in the quantum region may further improve this results, as was observed by Fahleson *et al.*[29]. This is likely due to the slow convergence of the magnetic transition dipole moment, compared to the electric transition dipole moment, with respect to the number of solvent molecules included in the quantum region.[36] When inspecting the intensity at peak maxima (Table 1) we observe that the continuum-model based results, both with and without cavity field effects, lead to overestimations. The corresponding intensities based on the explicit representation of the solvent are, on the other hand, in much better agreement with experiment. However, we observe that the PE

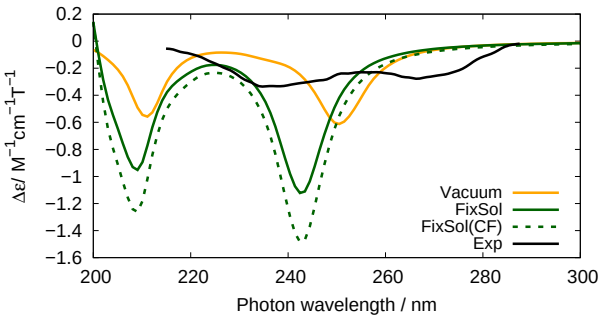

Fig. 2 The MCD spectrum of cytosine computed for a single optimized structure in gas phase and in water solution approximated by a continuum model (FixSol). Experimental spectrum in water by Voelter *et al.*[63]

model in general performs better than the standard water model TIP3P, thus highlighting the need to include an explicit representation of the solvent, and potentially polarization effects. When considering the EEF effects incorporated in the PE model we, for this system, do not observe a significant effect. As for the dielectric continuum model, the EEF effects in the PE model only affect the intensities of the signal. We find that the lowest electronic excitation, which is dominated by a HOMO-LUMO transition, is most sensitive to inclusion of EEF effects, with a resulting decrease in intensity from -0.41 to -0.36 $\mathrm{M^{-1}cm^{-1}T^{-1}}$.

4.2 Hypoxanthine

The second molecule to be considered is hypoxanthine. The MCD spectra of hypoxanthine in aqueous solution (at pH 6) displays a biphasic profile, i.e. opposite signs between the two electronic transitions in the absorption profile.[65] In Figure 4 the experimental spectrum is plotted together with the calculated spectra using a single optimized structure and a continuum approach (FixSol) to approximate the environmental effects. First, we observe a significant effect from the environment on both the positive and negative signal as compared to the vacuum results. Especially at peak maxima (see Table 2) the intensity of the MCD signal when going from vacuum to solution is more than doubled for both peak maxima. Also for hypoxanthine this enhancement is slightly increased when including the CF effects compared to the results based on the continuum approach excluding CF effects. Furthermore, as was the case for

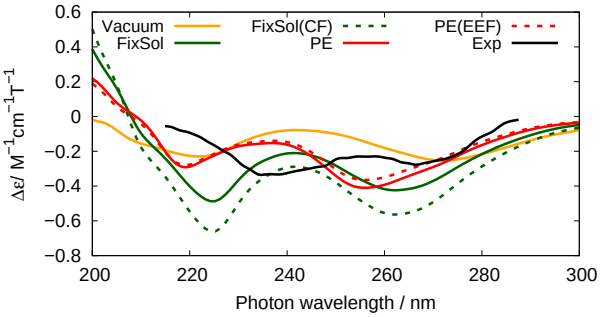

Fig. 3 The MCD spectrum of cytosine averaged over 100 snapshots in gas phase and in water solution approximated with both PE and continuum model (FixSol). Experimental spectrum in water by Voelter *et al.*[63]

Table 1 Line position and intensity of peak maxima and the energy separation between the two peaks of the MCD spectrum of cytosine. As detailed in the SI file, the standard errors of the mean (SEM) are in all cases between 0.01-0.06 $M^{-1}cm^{-1}T^{-1}$.

Environment	peak maxima/ eV	peak separation/ eV	Intensity at peak maxima/ $M^{-1}cm^{-1}T^{-1}$
Vac.[a]	4.94	0.94	−0.56
	5.88		−0.63
FixSol/CF[a,c]	5.10	0.83	−0.95/−1.25
	5.93		−1.13/−1.49
Vac.[b]	4.53	1.01	−0.24
	5.54		−0.27
PE/EEF[b,c]	4.86	0.80	−0.41/−0.36
	5.66		−0.30/−0.29
TIP3P[b]	4.79	0.82	−0.32
	5.61		−0.32
FixSol/CF[b,c]	4.73	0.78	−0.42/−0.56
	5.51		−0.50/−0.66
Exp[d]	4.67	0.58	−0.35
	5.25		−0.27

[a] Cytosine MCD spectrum based on a single geometry
[b] Cytosine MCD spectrum averaged over 100 snapshots
[c] Results seperated by / indicates inclusion of cavity field effects or external field effects
[d] Ref. [63]

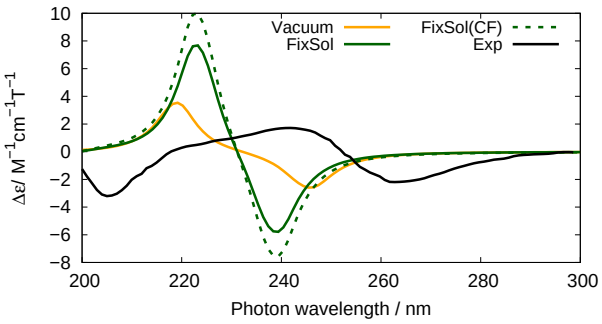

Fig. 4 The MCD spectrum of hypoxanthine computed for a single optimized structure in gas phase and in water solution approximated by a continuum model (FixSol). Experimental spectrum in water by Sutherland and Griffin.[65]

the cytosine molecule, the results for hypoxanthine show a general blue shift in peak position, compared to the experimental spectrum. However, the peak separation is greatly improved when including solvent effects, from 0.62 eV in vacuum to 0.37 eV in solution.

In Figure 5 we show the computed spectra of hypoxanthine averaged over 100 snapshots extracted from the MD simulation and using different solvation models. Again, as was the case for cytosine, the averaged spectra show much better agreement with experiment regarding both peak separation and computed intensities. Comparing directly the performance of the continuum approach based on the use of a single optimized structure to the similar but averaged results, the intensities for the negative signal decrease from -7.7 to -2.7 $\mathrm{M^{-1}cm^{-1}T^{-1}}$, while the positive signal intensities decrease from 10 to 4.1 $\mathrm{M^{-1}cm^{-1}T^{-1}}$. In both cases this is more in line with the experimental values, thus highlighting the importance of not only solvent dynamical effects, but also the finite temperature effects of the solute. For the PE model the peak separation is in perfect agreement with experiment: 0.42 eV compared to the experimental value of 0.43 eV. Furthermore, as seen from Figure 5, EEF effects play only a minor role in this case.

5 Conclusions

In this paper we have investigated the performance of the the Polarizable Embedding (PE) approach for calculating the MCD spectra of cytosine and hypoxanthine. To predict key MCD parameters of solvated molecules, it is im-

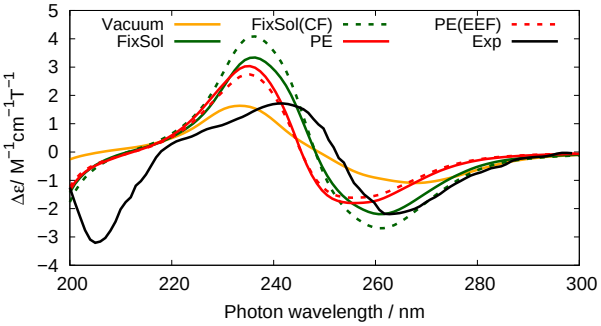

Fig. 5 The MCD spectrum of hypoxantine averaged over 100 snapshots in gas phase and in water solution approximated with both PE and continuum model (FixSol). Experimental spectrum in water by Sutherland and Griffin.[65]

Table 2 Line position and intensity of peak maxima and the energy separation between the two peaks of the MCD spectrum of hypoxanthine. As detailed in the SI file, the standard errors of the mean (SEM) are all below 0.35 $M^{-1}cm^{-1}T^{-1}$.

Environment	peak maxima/ eV	peak separation/ eV	Intensity at peak maxima/ $M^{-1}cm^{-1}T^{-1}$
Vac.[a]	5.04	0.62	−2.9
	5.66		3.5
FixSol/CF[a,c]	5.19	0.37	−5.9/−7.7
	5.56		7.5/10
Vac.[b]	4.63	0.67	−1.0
	5.30		1.6
PE/EEF[b,c]	4.86	0.42	−1.8/−1.6
	5.28		3.0/2.8
TIP3P[b]	4.81	0.49	−1.4
	5.30		2.4
FixSol/CF[b,c]	4.75	0.50	−2.0/−2.7
	5.25		3.3/4.1
Exp[d]	4.68	0.43	−2.1
	5.11		1.7

[a] Hypoxanthine MCD spectrum based on a single geometry
[b] Hypoxanthine MCD spectrum averaged over 100 snapshots
[c] Results seperated by / indicates inclusion of cavity field effects or external field effects
[d] Ref. [65]

portant that the method used is able to correctly account for medium effects. In order to account for this we have considered PE calculations both with and without EEF effects, and compared these to a continuum approach taking into account the cavity field effects. Our results show that the computationally most efficient model, i.e. optimizing a single molecular structure and accounting for solvation through a dielectric continuum model, is indeed capable of reproducing the main spectral features. However, the predicted intensities are significantly overestimated. Including both solvent and solute dynamics by considering a number of snapshots in the MCD calculations yields spectra that are in much better agreement with the experimental results. However, considering the averaged results we generally observe that intensities computed using a continuum approach are still overestimated compared to the experimental intensities and, furthermore, that inclusion of cavity field effects leads to a further enhancement of the signals. On the other hand, the PE model predicts both intensities and peak separations more in line with the experimental results than any of the models we have tested here.

Additional information

Structure files relevant for the project are available on Figshare (url: `https://figshare.com/projects/Modeling_Magnetic_Circular_Dichroism_within_the_polarizable_Embedding_Approach/27769`)

Acknowledgements Computational resources were provided by the DeIC National HPC Center at the University of Southern Denmark through an Abacus 2.0 grant. J. K. thanks the Danish Council for Independent Research and the Villum Foundation for financial support. S. C. acknowledges support from DTU Chemistry. This paper is dedicated to Antonio Rizzo on the occasion of his 60 years birthday. We would all like to thank Antonio for his significant scientific contributions and for being an extremely kind person.

References

1. L.D. Barron, *Molecular light scattering and optical activity* (Cambridge University Press, 2004)
2. W.R. Mason, *A Practical Guide to Magnetic CIrcular Dichroims* (John Wiley and Sons Inc., 2007)
3. D.J. Caldwell, H. Eyring, *The Theory of Optical Activity* (Wiley-Interscience, 1971)
4. A. Buckingham, P. Stephens, Annu. Rev. Phys. Chem. **17**(1), 399 (1966)
5. P. Schatz, A. McCaffery, Quart. Rev., Chem. Soc. **23**(4), 552 (1969)
6. R. Serber, Phys. Rev. **41**(4), 489 (1932)
7. P. Stephens, Chem. Phys. Lett. **2**(4), 241 (1968)
8. P. Stephens, J. Chem. Phys. **52**(7), 3489 (1970)
9. P. Stephens, Annu. Rev. Phys. Chem. **25**(1), 201 (1974)
10. P. Stephens, Adv. Chem. Phys **35**, 197 (1976)
11. S. Coriani, P. Jørgensen, A. Rizzo, K. Ruud, J. Olsen, Chem. Phys. Lett. **300**(1), 61 (1999)
12. S. Coriani, C. Hättig, P. Jørgensen, T. Helgaker, J. Chem. Phys. **113**(9), 3561 (2000)
13. T. Kjærgaard, B. Jansík, P. Jørgensen, S. Coriani, J. Michl, J. Phys. Chem. A **111**(44), 11278 (2007)

14. M. Seth, T. Ziegler, A. Banerjee, J. Autschbach, S.J. van Gisbergen, E.J. Baerends, J. Chem. Phys. **120**(23), 10942 (2004)
15. M. Seth, T. Ziegler, J. Autschbach, J. Chem. Phys. **122**(9), 094112 (2005)
16. M. Seth, J. Autschbach, T. Ziegler, J. Chem. Theory Comput. **3**(2), 434 (2007)
17. M. Seth, T. Ziegler, Adv. Inorg. Chem. **62**, 41 (2010)
18. H. Solheim, L. Frediani, K. Ruud, S. Coriani, Theor. Chim. Acta. **119**(1), 231 (2008)
19. M. Seth, M. Krykunov, T. Ziegler, J. Autschbach, A. Banerjee, J. Chem. Phys. **128**(14), 144105 (2008)
20. M. Seth, M. Krykunov, T. Ziegler, J. Autschbach, J. Chem. Phys. **128**(23), 234102 (2008)
21. T. Kjærgaard, P. Jørgensen, A.J. Thorvaldsen, P. Sałek, S. Coriani, J. Chem. Theory Comput.
22. T. Kjærgaard, K. Kristensen, J. Kauczor, P. Jørgensen, S. Coriani, A.J. Thorvaldsen, J. Chem. Phys. **135**(2), 024112 (2011)
23. T. Kjærgaard, S. Coriani, K. Ruud, Wiley Interdiscip. Rev.: Comput. Mol. Sci. **2**(3), 443 (2012)
24. P. Norman, D.M. Bishop, H. Jørgen Aa. Jensen, J. Oddershede, J. Chem. Phys. **115**(22), 10323 (2001)
25. P. Norman, D.M. Bishop, H.J.A. Jensen, J. Oddershede, J. Chem. Phys. **123**(19), 194103 (2005)
26. H. Solheim, K. Ruud, S. Coriani, P. Norman, J. Chem. Phys. **128**, 094103 (2008)
27. H. Solheim, K. Ruud, S. Coriani, P. Norman, J. Phys. Chem. A **112**(40), 9615 (2008)
28. T. Fahleson, J. Kauczor, P. Norman, S. Coriani, Mol. Phys. **111**(9-11), 1401 (2013)
29. T. Fahleson, J. Kauczor, P. Norman, F. Santoro, R. Improta, S. Coriani, J. Phys. Chem. A **119**(21), 5476 (2015)
30. M. Krykunov, M. Seth, T. Ziegler, J. Autschbach, J. Chem. Phys. **127**(24), 244102 (2007)
31. F. Santoro, R. Improta, T. Fahleson, J. Kauczor, P. Norman, S. Coriani, Phys. Chem. Lett. **5**(11), 1806 (2014)
32. L. Martinez-Fernandez, T. Fahleson, P. Norman, F. Santoro, S. Coriani, R. Improta, Photochem. Photobiol. Sci. (2017)
33. C.M. Isborn, B.D. Mar, B.F. Curchod, I. Tavernelli, T.J. Martinez, J. Phys. Chem. B **117**(40), 12189 (2013)
34. J.M. Milanese, M.R. Provorse, E. Alameda Jr, C.M. Isborn, J. Chem. Theory Comput.
35. D. Flaig, M. Beer, C. Ochsenfeld, J. Chem. Theory Comput. **8**(7), 2260 (2012)
36. M.S. Nørby, J.M.H. Olsen, C. Steinmann, J. Kongsted, J. Chem. Theory Comput. (2017)
37. A. Warshel, M. Levitt, J. Mol. Biol. **103**(2), 227 (1976)
38. J.M. Olsen, K. Aidas, J. Kongsted, J. Chem. Theory Comput. **6**(12), 3721 (2010)
39. J.M.H. Olsen, J. Kongsted, Adv. Quantum Chem **61**, 107 (2011)
40. M.N. Pedersen, E.D. Hedegård, J.M.H. Olsen, J. Kauczor, P. Norman, J. Kongsted, J. Chem. Theory Comput. **10**(3), 1164 (2014)
41. F. Lipparini, C. Cappelli, V. Barone, J. Chem. Phys. **138**(23), 234108 (2013)
42. T. Giovannini, M. Olszowka, F. Egidi, J.R. Cheeseman, G. Scalmani, C. Cappelli, J. Chem. Theory Comput. **13**(9), 4421 (2017)
43. P.N. Day, J.H. Jensen, M.S. Gordon, S.P. Webb, W.J. Stevens, M. Krauss, D. Garmer, H. Basch, D. Cohen, J. Chem. Phys. **105**(5), 1968 (1996)
44. M.S. Gordon, M.A. Freitag, P. Bandyopadhyay, J.H. Jensen, V. Kairys, W.J. Stevens, J. Phys. Chem. A **105**(2), 293 (2001)
45. P. Soderhjelm, C. Husberg, A. Strambi, M. Olivucci, U. Ryde, J. Chem. Theory Comput. **5**(3), 649 (2009)
46. M.S. Gordon, Q.A. Smith, P. Xu, L.V. Slipchenko, Annu. Rev. Phys. Chem. **64**, 553 (2013)
47. U.C. Singh, P.A. Kollman, J. Comp. Chem. **7**(6), 718 (1986)
48. M.A. Thompson, G.K. Schenter, J. Phys. Chem. **99**(17), 6374 (1995)
49. M.A. Thompson, J. Phys. Chem. **100**(34), 14492 (1996)
50. D. Bakowies, W. Thiel, J. Phys. Chem. **100**(25), 10580 (1996)
51. R.A. Bryce, R. Buesnel, I.H. Hillier, N.A. Burton, Chem. Phys. Lett. **279**(5-6), 367 (1997)

52. L. Jensen, P.T. van Duijnen, J.G. Snijders, J. Chem. Phys. **118**(2), 514 (2003)
53. J. Kongsted, A. Osted, K.V. Mikkelsen, O. Christiansen, J. Phys. Chem. A **107**(14), 2578 (2003)
54. C.J. Illingworth, S.R. Gooding, P.J. Winn, G.A. Jones, G.G. Ferenczy, C.A. Reynolds, J. Phys. Chem. A **110**(20), 6487 (2006)
55. C.B. Nielsen, O. Christiansen, K.V. Mikkelsen, J. Kongsted, J. Chem. Phys. **126**(15), 154112 (2007)
56. D.P. Geerke, S. Thiel, W. Thiel, W.F. van Gunsteren, J. Chem. Theory Comput. **3**(4), 1499 (2007)
57. C. Curutchet, A. Muñoz-Losa, S. Monti, J. Kongsted, G.D. Scholes, B. Mennucci, J. Chem. Theory Comput. **5**(7), 1838 (2009)
58. F. Lipparini, V. Barone, J. Chem. Theory Comput. **7**(11), 3711 (2011)
59. F. Lipparini, C. Cappelli, V. Barone, J. Chem. Theory Comput. **8**(11), 4153 (2012)
60. E. Boulanger, W. Thiel, J. Chem. Theory Comput. **8**(11), 4527 (2012)
61. C. Steinmann, J.M.H. Olsen, J. Kongsted, J. Chem. Theory Comput. **10**(3), 981 (2014)
62. T. Schwabe, M.T. Beerepoot, J.M.H. Olsen, J. Kongsted, Phys. Chem. Chem. Phys. **17**(4), 2582 (2014)
63. W. Voelter, R. Records, E. Bunnenberg, C. Djerassi, J. Am. Chem. Soc. **90**(22), 6163 (1968)
64. J.C. Sutherland, B. Holmquist, Annu. Rev. Biophys. Bioeng. **9**(1), 293 (1980)
65. J.C. Sutherland, K. Griffin, Biopolymers **23**(12), 2715 (1984)
66. J. Tomasi, B. Mennucci, R. Cammi, Chem. Rev. **105**(8), 2999 (2005)
67. N.H. List, H.J.A. Jensen, J. Kongsted, Phys. Chem. Chem. Phys. **18**(15), 10070 (2016)
68. L.J. Nåbo, N.H. List, C. Steinmann, J. Kongsted, J. Chem. Theory Comput. **13**(2), 719 (2017)
69. N.M. Thellamurege, H. Li, J. Chem. Phys. **137**(24), 246101 (2012)
70. A. Klamt, G. Schüürmann, J. Chem. Soc., Perk. Trans. 2 (5), 799 (1993)
71. E.V. Stefanovich, T.N. Truong, Chem. Phys. Lett. **244**(1), 65 (1995)
72. T.N. Truong, E.V. Stefanovich, Chem. Phys. Lett. **240**(4), 253 (1995)
73. V. Barone, M. Cossi, J. Phys. Chem. A **102**(11), 1995 (1998)
74. A. Klamt, J. Phys. Chem. **99**(7), 2224 (1995)
75. J. Kauczor, P. Jørgensen, P. Norman, J. Chem. Theory Comput. **7**(6), 1610 (2011)
76. J. Kauczor, P. Norman, J. Chem. Theory Comput. **10**(6), 2449 (2014)
77. J. Olsen, P. Jo/rgensen, J. Chem. Phys. **82**(7), 3235 (1985)
78. K. Aidas, C. Angeli, K.L. Bak, V. Bakken, R. Bast, L. Boman, O. Christiansen, R. Cimiraglia, S. Coriani, P. Dahle, E.K. Dalskov, U. Ekström, T. Enevoldsen, J.J. Eriksen, P. Ettenhuber, B. Fernández, L. Ferrighi, H. Fliegl, L. Frediani, K. Hald, A. Halkier, C. Hättig, H. Heiberg, T. Helgaker, A.C. Hennum, H. Hettema, E. Hjertenaes, S. Høst, I.M. Høyvik, M.F. Iozzi, B. Jansík, H.J.A. Jensen, D. Jonsson, P. Jørgensen, J. Kauczor, S. Kirpekar, T. Kjaergaard, W. Klopper, S. Knecht, R. Kobayashi, H. Koch, J. Kongsted, A. Krapp, K. Kristensen, A. Ligabue, O.B. Lutnaes, J.I. Melo, K.V. Mikkelsen, R.H. Myhre, C. Neiss, C.B. Nielsen, P. Norman, J. Olsen, J.M.H. Olsen, A. Osted, M.J. Packer, F. Pawlowski, T.B. Pedersen, P.F. Provasi, S. Reine, Z. Rinkevicius, T.A. Ruden, K. Ruud, V.V. Rybkin, P. Sałek, C.C.M. Samson, A.S. de Merás, T. Saue, S.P.A. Sauer, B. Schimmelpfennig, K. Sneskov, A.H. Steindal, K.O. Sylvester-Hvid, P.R. Taylor, A.M. Teale, E.I. Tellgren, D.P. Tew, A.J. Thorvaldsen, L. Thøgersen, O. Vahtras, M.A. Watson, D.J.D. Wilson, M. Ziolkowski, H. Ågren, Wiley Interdiscip. Rev.: Comput. Mol. Sci. **4**(3), 269 (2013)
79. J.M.H. Olsen. PElib: The Polarizable Embedding library (development version) (2014). Https://gitlab.com/pe-software/pelib-public
80. B. Gao. Gen1Int Version 0.3.0 (2014). Http://repo.ctcc.no/projects/gen1int
81. B. Gao, A.J. Thorvaldsen, K. Ruud, Int. J. Quantum Chem. **111**(4), 858 (2010)
82. A.D. Becke, J. Chem. Phys. **98**(7), 5648 (1993)
83. S.H. Vosko, L. Wilk, M. Nusair, Can. J. Phys. **58**(8), 1200 (1980)
84. C. Lee, W. Yang, R.G. Parr, Phys. Rev. B **37**(2), 785 (1988)
85. M.J. Frisch, G.W. Trucks, H.B. Schlegel, G.E. Scuseria, M.A. Robb, J.R. Cheeseman, G. Scalmani, V. Barone, B. Mennucci, G.A. Petersson, H. Nakatsuji, M. Caricato, X. Li, H.P. Hratchian, A.F. Izmaylov, J. Bloino, G. Zheng, J.L. Sonnenberg, M. Hada,

M. Ehara, K. Toyota, R. Fukuda, J. Hasegawa, M. Ishida, T. Nakajima, Y. Honda, O. Kitao, H. Nakai, T. Vreven, J.A. Montgomery, Jr., J.E. Peralta, F. Ogliaro, M. Bearpark, J.J. Heyd, E. Brothers, K.N. Kudin, V.N. Staroverov, R. Kobayashi, J. Normand, K. Raghavachari, A. Rendell, J.C. Burant, S.S. Iyengar, J. Tomasi, M. Cossi, N. Rega, J.M. Millam, M. Klene, J.E. Knox, J.B. Cross, V. Bakken, C. Adamo, J. Jaramillo, R. Gomperts, R.E. Stratmann, O. Yazyev, A.J. Austin, R. Cammi, C. Pomelli, J.W. Ochterski, R.L. Martin, K. Morokuma, V.G. Zakrzewski, G.A. Voth, P. Salvador, J.J. Dannenberg, S. Dapprich, A.D. Daniels, V. Farkas, J.B. Foresman, J.V. Ortiz, J. Cioslowski, D.J. Fox. Gaussian09 Revision D.01. Gaussian Inc. Wallingford CT 2009

86. D.A. Case, R. Betz, D.S. Cerutti, T.E. Cheatham, III, T.A. Darden, R.E. Duke, T.J. Giese, H. Gohlke, A.W. Goetz, N. Homeyer, S. Izadi, P. Janowski, J. Kaus, A. Kovalenko, T.S. Lee, S. LeGrand, P. Li, C. Lin, T. Luchko, R. Luo, B. Madej, D. Mermelstein, K.M. Merz, G. Monard, H. Nguyen, H.T. Nguyen, I. Omelyan, A. Onufriev, D. Roe, A. Roitberg, C. Sagui, C.L. Simmerling, W.M. Botello-Smith, J. Swails, R.C. Walker, J. Wang, R.M. Wolf, X. Wu, L. Xiao, P.A. Kollman. AMBER 2016 (2016)
87. M. Korth, J. Chem. Theory Comput. **6**(12), 3808 (2010)
88. W.L. Jorgensen, J. Am. Chem. Soc. **103**(2), 335 (1981)
89. W.L. Jorgensen, J. Chandrasekhar, J.D. Madura, R.W. Impey, M.L. Klein, J. Chem. Phys. **79**(2), 926 (1983)
90. T. Yanai, D.P. Tew, N.C. Handy, Chem. Phys. Lett. **393**(1), 51 (2004)
91. T.H. Dunning, J. Chem. Phys. **90**(2), 1007 (1989)
92. L. Gagliardi, R. Lindh, G. Karlström, J. Chem. Phys. **121**(10), 4494 (2004)
93. O. Vahtras. Loprop for dalton (2014). URL `http://dx.doi.org/10.5281/zenodo.13276`
94. A. Kaito, M. Hatano, T. Ueda, S. Shibuya, Bull. Chem. Soc. Jpn. **53**(11), 3073 (1980)